Singlet ground-state fluctuations in praseodymium observed by muon spin relaxation in PrP and $PrP_{0.9}$

2005 J. Phys.: Condens. Matter 17 119

(http://iopscience.iop.org/0953-8984/17/1/012)

INSTITUTE OF PHYSICS PUBLISHING JOURNAL OF PHYSICS: CONDENSED MATTER

J. Phys.: Condens. Matter **17** (2005) 119–136 doi:10.1088/0953-8984/17/1/012

Singlet ground-state fluctuations in praseodymium observed by muon spin relaxation in PrP and $PrP_{0.9}$

D R Noakes[1], R Wäppling[2], G M Kalvius[3], M F White Jr[1] and C E Stronach[1]

[1] Chemistry and Physics Department, Virginia State University, Petersburg, VA 23806, USA
[2] Physics Department, Uppsala University, S-751 21 Uppsala, Sweden
[3] Physik Department-E15, Technische Universität München, D-85747 Garching, Germany

Received 25 June 2004, in final form 19 November 2004
Published 10 December 2004
Online at stacks.iop.org/JPhysCM/17/119

Abstract
Muon spin relaxation (μSR) in the singlet ground-state compounds PrP and $PrP_{0.9}$ reveals the unusual situation of a Lorentzian local field distribution with fast-fluctuation-limit strong-collision dynamics, a case that does not show motional narrowing. Contrary to publications by others, where $PrP_{0.9}$ was asserted to have vacancy-induced spin-glass freezing, no spin-glass freezing is seen in $PrP_{0.9}$ or PrP down to $\lesssim$100 mK. This was confirmed by magnetization measurements on these same samples. In both compounds, the muon spin relaxation rate does increase as temperature decreases, demonstrating increasing strength of the paramagnetic response. A Monte Carlo model of fluctuations of Pr ions out of their crystalline-electric-field singlet ground states into their magnetic excited states (and back down again) produces the strong-collision-dynamic Lorentzian relaxation functions observed at each individual temperature but not the observed temperature dependence. This model contains no exchange interaction, and so predicts decreasing paramagnetic response as the temperature decreases, contrary to the temperature dependence observed. Comparison of the simulations to the data suggests that the exchange interaction is causing the system to approach magnetic freezing (by mode softening), but fails to complete the process.

Stoichiometric PrP is a non-magnetic, crystalline-electric-field (CEF) singlet ground-state system showing Van Vleck susceptibility and no magnetic ordering down to 1 K. Non-stoichiometric PrP_x ($0.85 < x < 0.95$) has been proposed as an 'induced moment spin glass' [1, 2], with freezing temperatures below 10 K. This stronger magnetism has been attributed to moments that are induced on Pr ions adjacent to phosphorus vacancies by the vacancies' disturbance of the CEF on those adjacent praseodymium ions. This paper describes transverse-field (TF), zero-field (ZF) and longitudinal-field (LF) muon spin relaxation (μSR) measurements on polycrystalline PrP and $PrP_{0.9}$. The data show qualitatively similar behaviour in the two materials, with no indication of spin-glass freezing. The μSR spectra are anomalous, however, in that they are best described by strong-collision dynamics on a Lorentzian field distribution, a model that had been considered unphysical, since it shows no motional narrowing (preliminary results were presented in [3]). We report Monte Carlo numerical simulations of a model involving fluctuations of the praseodymium ions out of the non-magnetic ground singlet into magnetic excited CEF states (and back down again), with dipole coupling to the muon magnetic moment. The model reproduces the observed μSR spectra at each individual temperature. Since the model does not contain exchange interaction effects, the non-magnetic singlet ground-state occupation increases as the temperature decreases. Consequently, the model predicts that the paramagnetism of the material will decrease in strength as the temperature is lowered, which would lead to decreasing muon relaxation rates with decreasing temperature. Contrary to this, we observed that the relaxation rate increases in both PrP and $PrP_{0.9}$ as the temperature is reduced. While remaining paramagnetic, and in fact strong-collision Lorentzian dynamic, nonetheless the magnetic response is strengthening as the temperature is reduced. The likely cause of this is the exchange interaction missing from the current Monte Carlo model, which causes an approach to magnetic ordering (within the context of the model, it looks like mode-softening of the CEF first excited state), without completing the process.

The following sections describe (1) some pertinent features of the μSR technique, (2) the observations from PrP_x, and the strong-collision dynamic Lorentzian Kubo–Toyabe relaxation functions that fit them, (3) the Monte Carlo singlet ground fluctuation model, (4) how the model reproduces the observations at individual temperatures, but fails to reproduce the temperature dependence, (5) an unsuccessful comparison model that is more like the vacancy-induced-moment model of [1, 2], to show that these simulations allow discrimination between various models, and (6) discussion and conclusions.

1. The muon spin relaxation technique

The experimental details of muon spin relaxation measurements are reviewed in detail in, for example, [4–6]. In a standard time-differential 'surface muon' μSR measurement, a beam of 4 MeV positive muons of nearly 100% polarization is delivered to the sample of interest, usually mounted in a cryostat in the centre of Helmholtz-type coils allowing the application of static magnetic fields. The passage of a muon into the sample is detected by a thin counter in front of the sample, which starts a clock. The beam intensity is limited, and vetoes set, so that data are recorded only when there is only one muon in the sample at a time. Each muon thermalizes instantaneously (on the timescale of the muon lifetime of 2.2 μs) without loss of polarization, usually coming to rest (in metallic solids below room temperature) at an interstitial site far from any damage it might have caused during thermalization. The muon magnetic moment then interacts with the magnetic moments in the material until it decays. The decay positron is emitted preferentially (asymmetrically) in the direction the muon magnetic moment was pointing at the instant of decay. Positron detectors arrayed around the sample detect the direction and time since the muon stop, and a histogram of events as a function of time $N(t)$ in that direction is incremented. A typical measurement involves one to ten million muon-in/positron-out events.

For zero field (ZF) and longitudinal field (LF) μSR spectra, positron counters are placed backward (B) and forward (F) with respect to the initial muon polarization. These generate histograms of counts as a function of time $N_B(t)$ and $N_F(t)$. The random background is measured and subtracted as described in [7] to obtain the background-corrected histograms $N'_B(t)$ and $N'_F(t)$. One then can define the 'raw asymmetry'

$$A_{raw}(t) \equiv \frac{N'_B(t) - N'_F(t)}{N'_B(t) + N'_F(t)}, \quad (1)$$

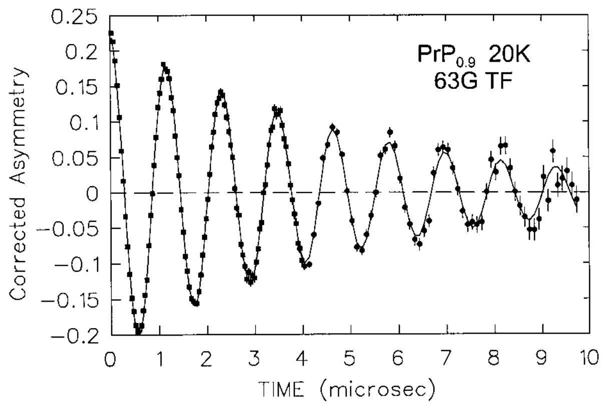

Figure 1. 63 G TF-μSR asymmetry spectrum from $PrP_{0.9}$ at 20 K. The solid curve is the least-squares fit to a single-frequency signal with exponentially-relaxing envelope.

which in the case of ideally-identical counters would be equal to $A_0G(t)$, where A_0 is the initial (i.e., at $t = 0$) count rate asymmetry (whose value depends on the apparatus, being typically 0.2–0.3) and $G(t)$ is 'the muon spin relaxation function', the time dependence of the spin polarization of the muon ensemble due to the interaction with the fields acting at the muon site. In practice, the relative counting efficiency of the two positron detectors $\alpha = N_B(0)/N_F(0)$ is not equal to one, and in that case

$$A_0G(t) = \frac{(\alpha - 1) + (\alpha + 1)A_{\text{raw}}(t)}{(\alpha + 1) + (\alpha - 1)A_{\text{raw}}(t)} \equiv A(t). \tag{2}$$

$A(t)$ is called the 'corrected asymmetry'. In this way the quantity of interest $G(t)$ is deduced from the recorded time histograms $N(t)$.

The instrumental amplitude scale factor A_0 and relative efficiency α can be determined separately in a low-transverse-field (TF) μSR measurement. A field of a few tens of gauss (small enough that it does not significantly steer the incoming muon beam) perpendicular to the muon polarization (and beam travel direction) is applied to the sample. In the paramagnetic state, where the muon spin relaxation is usually slow, muon polarization will precess around the applied field at its Larmor frequency determined by the muon gyromagnetic ratio ($\gamma_\mu = 2\pi \times 13.55$ kHz $G^{-1} = 0.085\,14\,\mu s^{-1}\,G^{-1}$, assuming any paramagnetic frequency shift is negligible in such a small field) as it relaxes, creating oscillating $A(t)$ in the B and F counters. This is illustrated in figure 1 for our $PrP_{0.9}$ sample at 20 K in 63 G TF. Fitting with a relatively simple relaxing envelope (in this case, exponential) allows deduction of A_0 and α values, which apply also to ZF and LF spectra for the same sample, as long as the apparatus and sample are not disturbed. The analysis of TF-μSR data relies on the applied field being larger than most of the fields generated internally by the sample itself (the local fields are then perturbations to the applied field at the muon site). As electronic magnetism begins to appear in the sample, as the temperature is lowered, internal fields often become large, relaxation becomes fast, and TF measurements become difficult to interpret. ZF and LF are then advantageous, and are used more often to probe for details of magnetic states of materials.

In disordered magnetic materials, the interaction of the muons' magnetic moments with the surrounding magnetic moments is usually modelled by assuming that the magnetic material generates a probability distribution of the effective magnetic field $P(\mathbf{B})$ at the muon site (for reviews of the general phenomenology of μSR in magnetic materials, see [5, 6, 8]). For materials that are dense in magnetic moments (an average of at least one moment in the muon site's nearest-neighbour shell), the distribution of each field component is usually Gaussian to a good approximation. For dilute magnetic alloys, the distribution approaches Lorentzian (that is, the distribution of each Cartesian component of the local field approaches Lorentzian shape [9, 10]). When a muon stops, a single effective field is randomly chosen out of the distribution. If the local fields are static (as is often the case in magnetically ordered or frozen states), the muon moment precesses during its lifetime about its initial local field. With electronic moments in the paramagnetic state, however, the local field is usually dynamic, changing in magnitude and direction during the muon's lifetime. The simplest way to represent this is with a 'strong collision' model [11–13], where the local field is held constant between instantaneous hops (at an average rate $\nu_{\rm hop}$), and a new field is chosen randomly out of the distribution at each hop (there is then no correlation between the field before and the field after a jump). For a Gaussian field distribution in ZF and LF, this produces the 'dynamic Gaussian Kubo–Toyabe' relaxation function [14, 15], a workhorse in the analysis of μSR data in general.

Dynamic muon spin relaxation functions usually cannot be calculated in closed form for finite non-zero fluctuation rates $\nu_{\rm hop}$. Simple closed-form expressions are recovered in the 'fast-fluctuation' limit: in ZF, for a Gaussian distribution of local field with rms component field $B_{\rm rms}$,

$$G_{\rm G,ZF}(t) = \exp(-\lambda_{\rm G,ZF}t) = \exp\left(-\frac{2\Delta^2 t}{\nu_{\rm hop}}\right), \qquad \nu_{\rm hop} \gg \Delta, \tag{3}$$

where $\Delta \equiv \gamma_\mu B_{\rm rms}$. This exhibits 'motional narrowing', a term borrowed from NMR, where it is normal to work in frequency space (Fourier transform of time space), with applied (transverse) fields making all signals oscillate. The term then refers to the fact that the width of the NMR resonance is reduced as the motions of the spins increase [16]. The relaxation rate $\lambda_{\rm G,ZF} = 2\Delta^2/\nu_{\rm hop}$ goes to zero as $\nu_{\rm hop} \to \infty$.

If a longitudinal field $B_{\rm LF}$ is applied when the local fields are static, it competes with the local field distribution, tending to hold the muon polarization in its initial orientation while the local fields tend to rotate the muon spin. If the applied field is larger than typical local fields, significantly slower muon spin relaxation will be observed: the longitudinal field 'decouples' the muon from the local fields. When a longitudinal field is applied in the fast-fluctuation limit, however, it is well established that the relaxation function $G_{\rm G,LF}(t)$ is exponential, with relaxation rate

$$\lambda_{\rm G,LF} = \frac{\lambda_{\rm G,ZF}}{1+\omega_{\rm LF}^2/\nu_{\rm hop}^2}, \qquad \nu_{\rm hop} \gg \Delta, \tag{4}$$

where $\omega_{\rm LF} = \gamma_\mu B_{\rm LF}$ [16]. Thus there is little discernible LF decoupling until the applied-field Larmor frequency approaches the local field fluctuation rate. This usually requires quite large applied fields.

When the same strong-collision dynamics calculations are performed for a field distribution where the distribution of each Cartesian component B_i is Lorentzian and characterized by its half-width at half-maximum $B_{\rm hwhm}$ (because the rms-field integral diverges), the ZF relaxation function $G_{\rm L,ZF}(t)$ is again exponential in the fast-fluctuation limit, but with rate [17, 18]

$$\lambda_{\rm L,ZF} = \tfrac{4}{3}a, \qquad \nu_{\rm hop} \gg a, \tag{5}$$

where $a \equiv \gamma_\mu B_{\rm hwhm}$ ([17, 18] appear to disagree on this due to a typographical error in [18]). Here, the relaxation rate does not depend on the fluctuation rate and does not go to zero as $\nu_{\rm hop} \to \infty$, meaning that it does not show motional narrowing. The underlying cause is the Lorentzian field distribution's divergent second moment. In the strong collision model, this allows sufficient probability of arbitrarily large fields to counter the decoupling effect of multiple changes of local field.

The issue of identifying appropriate dynamics when the field distribution is Lorentzian emerged for μSR studies of classic dilute-alloy spin glasses, such as Cu(Mn), where ZF static Lorentzian Kubo–Toyabe relaxation is seen far below the freezing temperature T_f, but as the temperature is raised in the paramagnetic state, there is motional narrowing. Uemura and co-workers [19–21] developed a special model of local field dynamics for a stationary muon in a dilute alloy, noting that any particular muon will be a particular distance from the nearest ion moment, and then can experience only a limited range of fluctuating fields out of the complete Lorentzian distribution. They modelled this by assuming that each muon sees a Gaussian distribution, with a particular width Δ, of fluctuating fields during its lifetime, but that different muons randomly choose different Δ values out of a distribution of field widths constructed so that the complete field distribution summed over all muons is Lorentzian. There is then motional narrowing, but in the fast-fluctuation limit, the ZF relaxation function is not simple exponential, it is 'root exponential':

$$G_{\mathrm{ZF}}^{\mathrm{sg}}(t) = \exp\left(-\sqrt{4a^2 t/\nu_{\mathrm{hop}}}\right), \qquad \nu_{\mathrm{hop}} \gg a. \tag{6}$$

This motionally narrows, but more slowly than the Gaussian case. If a longitudinal field is applied in the fast-fluctuation limit, decoupling does not follow equation (4), but is as described in [22].

The field-decoupling behaviour of the true Lorentzian distribution without motional narrowing (i.e., a Lorentzian analogue of equation (4)) has not been pursued to date because the need had not arisen. This case will be discussed in the next section with particular reference to PrP_x.

2. Muon spin relaxation in PrP_x

The phase purity of the samples was checked using x-ray diffractometry. In the PrP samples, traces of PrP_2 are a consequence of maximizing the phosphorus content, while the under-stoichiometric samples contained no PrP_2 and had lattice constants consistent with $PrP_{0.9}$. μSR measurements were performed using 'surface muon' beam lines at TRIUMF.

Transverse field μSR runs were taken in 63 G field down to 4.0 K in PrP and 12.0 K in $PrP_{0.9}$. An example is shown in figure 1. In addition to measuring A_0 and α, they provided an indication of the qualitative behaviour. While the materials are semiconducting, and muonium often forms in semiconductors, the TF frequency is characteristic for a 'bare' muon. Evidence of muonium in the presence of electronic moments in semiconductors is rare, because spin-exchange fluctuations decouple the muonium hyperfine interaction (see [23]). TF relaxation was exponential at all temperatures measured, with rates as shown in figure 2. Note that the relaxation rate in $PrP_{0.9}$ is always higher than in PrP at the same temperature, consistent with $PrP_{0.9}$ being more magnetic, but the qualitative form of the behaviour is the same in the two materials. The increase in relaxation rates at low temperatures seems to begin around 70 K, far above any proposed spin-glass freezing. Instead, this temperature is in the range of the first excited CEF levels (4 and 8 meV above the non-magnetic ground state) reported by inelastic neutron scattering [2]. The exponential TF relaxation-envelope shape could be caused by a Lorentzian local field distribution, or by fast fluctuations in a Gaussian field distribution. To distinguish between these possibilities, we look to ZF and LF-μSR.

Typical ZF and LF asymmetry spectra from our two samples are shown in figure 3. Muon spin relaxation in ZF was also exponential at all temperatures investigated, increasing slowly

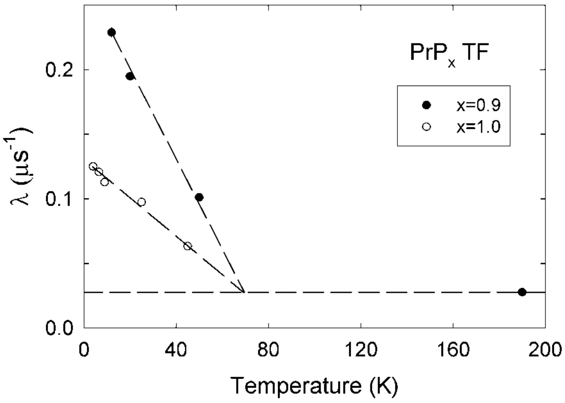

Figure 2. Exponential muon spin relaxation rates in PrP and $PrP_{0.9}$ in 63 G TF, as functions of temperature. The dashed lines are guides for the eye.

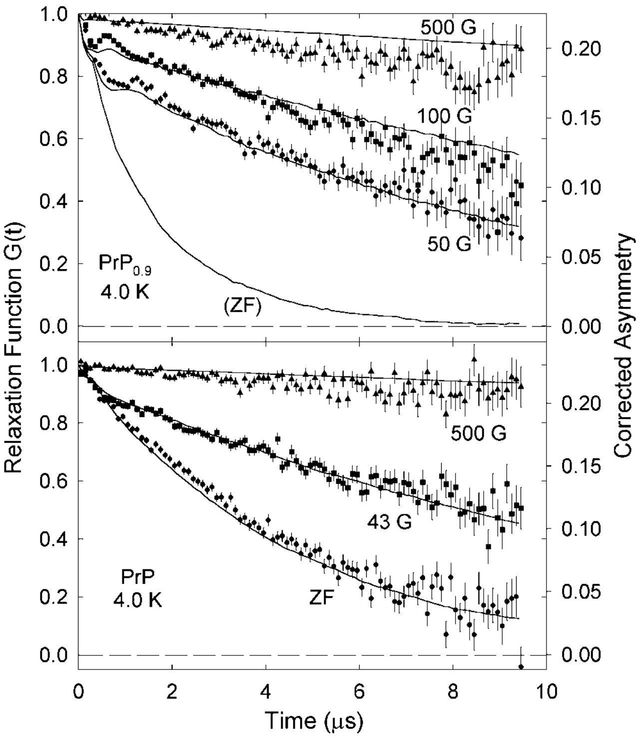

Figure 3. ZF and LF (at the fields indicated) μSR asymmetry spectra at 4.0 K in $PrP_{0.9}$ (top panel) and PrP (bottom panel). The solid curves show Monte Carlo simulations of the CEF-state fluctuation model described in the text. For $PrP_{0.9}$, no ZF data were taken at this temperature, but the model expectation for ZF is shown.

in rate as the temperature decreased, with, again, the rate always slightly larger in $PrP_{0.9}$ at the same temperature. There was no indication of any spin freezing down to the lowest temperatures measured (~60 mK): both samples appear to remain paramagnetic. Since this is contrary to statements in the literature, we also performed magnetization measurements on these samples. The results are shown in figure 4, as a function of temperature at 1000 Oe, and as a function of field at 10 K. The behaviour is basically paramagnetic, with no indication of a freezing temperature (in the magnetization) down to 5 K.

Exponential ZF relaxation is usually an indication of the ‘fast-fluctuation limit’ described above, where the fluctuation rate of the local field at the muon site is much larger than the Larmor precession frequency in the typical local field. If the relatively slow (for electronic

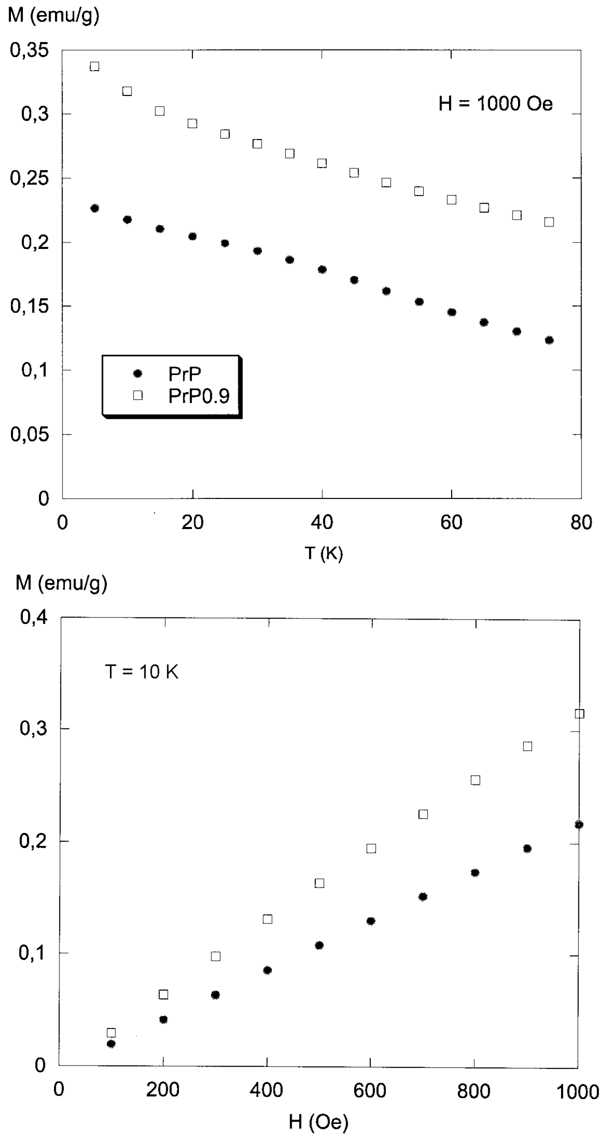

Figure 4. Magnetization data for the PrP (solid circles) and $PrP_{0.9}$ (open squares) samples used for the μSR measurements. The upper panel shows the temperature dependence in a field of 1000 Oe, while the lower panel shows the field dependence at 10 K.

moments) muon relaxation is due to very rapid fluctuations countering the effect of large local fields, then the application of LF would have little effect until the LF Larmor frequency approached the fluctuation rate, and even if some decoupling occurred, the relaxation function would remain exponential. In figure 3, it can clearly be seen that as little as 43 G LF causes partial decoupling (and it does so at every temperature measured), and 500 G results in nearly full decoupling. Further, there were some initial oscillations in the LF spectra. These effects suggest that the local fields at the muon site are only of the order of tens to hundreds of gauss, and the fluctuation rates can then be rather slow for electronic moments.

Neither the dynamic Gaussian Kubo–Toyabe function nor the Uemura dynamic spin-glass relaxation function fits the exponential ZF relaxation and LF decoupling behaviour of the PrP_x data, at any temperature. As an example of this, figure 5 shows the least squares fit of the

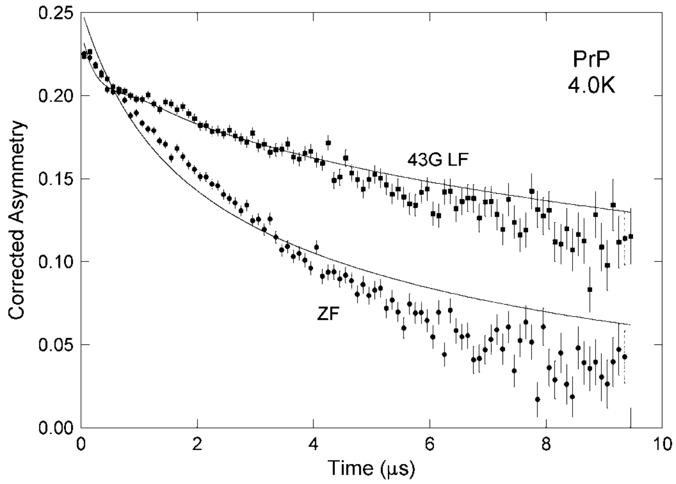

Figure 5. Simultaneous least-squares fit of the Uemura dynamic spin-glass relaxation function to ZF and 43 G LF μSR asymmetry spectra at 4.0 K in PrP (data from the bottom panel of figure 3) simultaneously. The quality of fit is unacceptably poor.

Uemura dynamic spin-glass function (as extended to LF by Keren [22]) to part of the data in the lower panel of figure 3. We consider this fit to be unacceptably poor.

The strong-collision dynamic Lorentzian Kubo–Toyabe function had been previously calculated numerically for low LF and low fluctuation rates [24]. As mentioned, the complete spectrum of behaviour with fluctuations, right up to LF decoupling in the fast-fluctuation limit, had not been considered. We ran the same numerical calculations (with thanks to J H Brewer for giving us his code) to high LF and fluctuation rate (relative to Lorentzian width a), and found that exponential relaxation fitted the simulated behaviour at sufficiently high field and fluctuation rate. Plotting the deduced exponential relaxation rate $\lambda_{L,LF}$ as a function of fluctuation rate ν_{hop} and applied-field Larmor frequency ω_{LF}, we found that $\lambda_{L,LF}$ does not obey equation (4). Instead, we found that it is described very well by

$$\lambda_{L,LF} = \frac{\lambda_{L,ZF}}{\sqrt{1+\omega_{LF}^2/\nu_{hop}^2}}, \qquad \nu_{hop} \gg a. \tag{7}$$

The complete simulated strong-collision dynamic Lorentzian Kubo–Toyabe function was incorporated into a standard program for least-squares fitting of μSR data, and we found that it fitted well (and consistently better than the alternatives) all the ZF- and LF-μSR observed in PrP and $PrP_{0.9}$, as described in our preliminary paper [3]. Those fits characterized the data in terms of two temperature-dependent parameters: the Lorentzian relaxation rate a (as defined after equation (5)), whose deduced values are shown in figure 6, and the fluctuation rate of the local field ν_{hop} (which was roughly constant around 1.2 μs^{-1}).

In the next section, a physically reasonable model of fluctuations of praseodymium moments in PrP_x will be presented. ZF and LF muon spin relaxation functions directly calculated with this model will be seen to be consistent with equation (7), and with the μSR data observed from these materials, indicating that PrP_x is a system generating strong-collision dynamic Lorentzian Kubo–Toyabe muon spin relaxation.

3. The CEF singlet ground state fluctuation model

The fact that the strong-collision-dynamic Lorentzian Kubo–Toyabe function fits the PrP μSR data, and the Uemura spin-glass function does not, indicates that each muon in the material is able to sample the entirety of the field distribution. Technically, this might be achieved

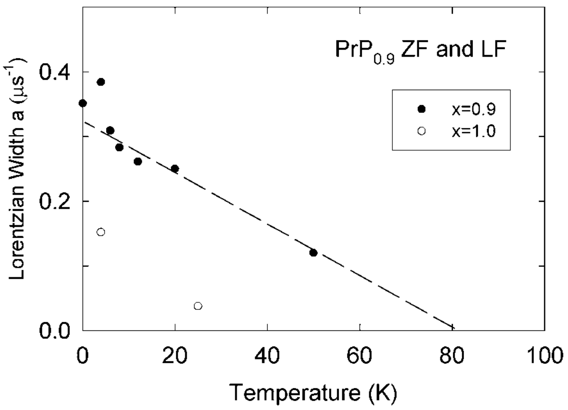

Figure 6. B_{hwhm} of the Lorentzian field distribution, expressed as the relaxation rate $a = \gamma_\mu B_{\mathrm{hwhm}}$, deduced from dynamic Lorentzian Kubo–Toyabe fits to ZF and LF-μSR in PrP and $PrP_{0.9}$.

by having muons not stopped, but diffusing in a dilute alloy. A muon initially far from a moment (low local field) then has a chance of moving near to a moment (high local field) within its lifetime, and *vice versa*. While muon diffusion over wide temperature ranges is observed in high-quality samples of many elements and binary semiconductors, strains and imperfections will generally prevent muon motion below ∼200 K (see, for example, [25]). We have therefore assumed that the muon is stationary in the material. If the ion moments in the material were stable, that is, fixed in magnitude even when varying in direction, then this would place each muon a fixed distance from the nearest moment, and the Uemura dynamic spin-glass function (which does not fit our data) would apply. With a singlet ground state, however, the praseodymium moment is not stable.

The ‘singlet ground state’ behaviour of PrP is a crystalline electric field (CEF) effect (for a review, see [26]). The praseodymium ion is usually in a 3+ charge state in a solid, with its f electrons collectively in a state of total angular momentum $J = 4$, with, in general, nine J_z sub-states. The multipole moments of the aspherical f-orbital charge cloud (which carries the magnetic moment) of each Pr interact with the multipole moments of the electric field at the ion site produced by the aspherical distribution of charged ions around it, creating nine energy states (the CEF states), which contain a mixture of different J_z and are separated in energy with respect to each other by up to tens or even hundreds of kelvins. An isolated singlet state is always non-magnetic, even though other CEF states grouped in multiplets can be magnetic. The ground state is a singlet in a number of Pr materials, including PrP, whose magnetic (non-singlet) first excited state is located at ∼130 K [1, 2]. At temperatures higher than this, the magnetic states are occupied, and the material displays fairly normal paramagnetism. Below this, however, the occupancy of the magnetic states drops, and the magnetic response fades (Van Vleck paramagnetism). In PrP_x, vacancies introduced by the under-stoichiometry are believed to reduce the first-excited-state energy of the Pr ions around each vacancy [1, 2] to the point where the exchange interaction (the cause of magnetic ordering in solids) can induce low-temperature moments and freezing of those few magnetic ions (although our observations indicate freezing does not occur in our samples). In PrP, then, a single Pr ion’s moment is zero when the ion is in the CEF ground state, but not zero when it is in a magnetic excited state. The moment switches on and off (flickers) as the ion’s electronic state fluctuates out of the CEF ground state into a higher, magnetic state and then back to the ground state. At temperatures well below the first excited state, only a small fraction of the Pr moments will be ‘on’ at any instant, providing the dilute-moment situation that generates a Lorentzian field distribution. Note that, in contrast to the usual cases, there is no chemical dilution of the moments in the

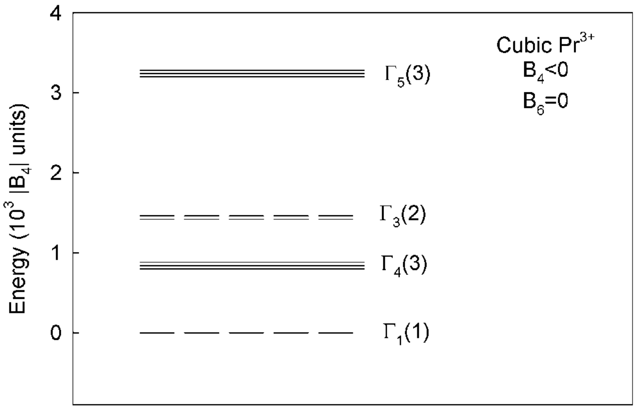

Figure 7. Pr^{3+} CEF energy levels in cubic PrP, in the approximation that B_6 is zero, as argued by [1]. The solid lines indicate magnetic states, and the dashed lines indicate non-magnetic states.

present case. A single stationary muon initially will be a particular distance away from a Pr that is 'on', but if the fluctuation rate between CEF-split levels is high enough, then either that moment will turn off, or another Pr ion closer to the muon will turn on during that muon's lifetime. The local field at the muon thus can easily go from very small to very large values (or vice versa), sampling the entire range of the Lorentzian field distribution, contrary to the Uemura spin-glass model, which applies for stable dilute moments.

To produce a numerical simulation of this, consider muons stopping in a perfect PrP lattice at finite temperature T, and a model of the magnetic moment changes caused by each Pr ion fluctuating between its CEF-split sub-states that must be taking place at some average rate per ion ν_{Pr}. Hasanain *et al* [1] argued that the cubic CEF in PrP is dominated by the Lea *et al* [27] B_4 parameter, and B_6 can be ignored. The B_n parameters have units of energy. In this case, there is a singlet ground state ($\Gamma_1(1)$, $E_0 \equiv 0$) whenever B_4 is negative. The first excited level is a ($\Gamma_4(3)$) triplet at $E_1 \cong 840\,|B_4|$ with a moment of $0.4\,\mu_{\mathrm{B}}$, beyond which there is a non-magnetic ($\Gamma_3(2)$) doublet at $E_2 \cong 1440\,|B_4|$ and a large-moment ($\Gamma_5(3)$) triplet at $E_3 \cong 3240\,|B_4|$. These energy levels are illustrated in figure 7. For PrP, B_4 is in the range -0.1 to -0.2 K, and for the temperatures of interest here ($\lesssim$50 K) the highest excited level is almost never occupied. The overwhelming preponderance of the magnetic behaviour comes from the first excited level. The Monte Carlo model of this paper considers not just a Boltzmann distribution of occupancies of these levels corresponding to the user-chosen temperature, but also fluctuations around the equilibrium configuration of the Pr ions surrounding a muon during its lifetime, preserving the Boltzmann distribution on average.

We have previously published results of Monte Carlo simulations of muon spin relaxation functions [10, 28] where local fields at the muon site are calculated by explicit summation of the dipole fields from moments on lattice clusters. In the earlier work, only static relaxation functions were simulated; here, ion moment dynamics creating dynamic local fields at the muon site are considered.

The cluster was a cube, with Pr ions placed as in the cubic PrP structure. For each muon event, a new distribution of the Pr ions' initially-occupied CEF states was constructed on the cluster at time $t = 0$. Initial level occupancy was assigned according to the Boltzmann distribution for the chosen temperature (for the Hasanain *et al* CEF model described above, distinctive behaviour is determined by the dimensionless ratio $kT/\,|B_4|$, or more intuitively, $kT/E_1 = kT/(840\,|B_4|)$). Moments were assigned only to Pr ions in state E_1 or E_3 (when the latter occurred, which was rare). Moment magnitude was assigned as listed above, while the moment direction was random. Both the interstitial $(\frac{1}{2}, \frac{1}{2}, \frac{1}{2})$ and the phosphorus ion site (representing the muon occupying a P vacancy) were evaluated (the difference, for the dynamic relaxation functions, was very small). The local field at the muon site was evaluated by a dipole sum over the cluster. When simulating a LF spectrum, the applied field vector $\mathbf{B}_{LF}$ was added to the summed local field $\mathbf{B}_{loc}$. The muon spin precessed about the resulting total $\mathbf{B}$ as a fixed field until a fluctuation occurred somewhere in the cluster.

Fluctuations were treated as completely incoherent random-time events with average rate per ion ν_{Pr} chosen by the user. In reality, fluctuations between CEF-split sub-states are controlled by complex, material-dependent properties such as the phonon spectrum and spin–lattice coupling, proper modelling of which are beyond the scope of this work (if possible at all). In an early work [7], ν as a function of T was parameterized using a CEF level scheme and a number of simplifying assumptions, and then fitted to results of ZF-μSR in $SmRh_4B_4$ and $ErRh_4B_4$, but in that case the absolute fluctuation rate could not be deduced even for the field at the muon site (ν_{hop}), much less for the rare earths ($\nu_{Sm,Er}$) themselves. Here the moment fluctuation process is modelled in more detail, but ν_{Pr} is a parameter adjusted independently of T in trying to reproduce the ZF and LF-μSR spectra observed in PrP.

At the time selected by the Monte Carlo procedure (using the given value of ν_{Pr}) for the first fluctuation to occur in the cluster, a Pr ion is selected at random, and, given its initial level E_i, the probability of transition to a particular other level $E_{j\neq i}$ is calculated as

$$P_{tr}(E_i \to E_{j\neq i}) = \frac{\exp((E_i - E_j)/2kT)}{\sum_{k\neq i}\exp((E_i - E_k)/2kT)}. \quad (8)$$

Note that equation (8) does not describe a rate, nor any time dependence. It describes the probabilities of how a state has changed, once it is known that it has changed. The complete single-ion state-to-state fluctuation rate expression is

$$\nu_{i\to j}(E_i \to E_{j\neq i}) = \nu_{Pr}(T)\left[\frac{1}{Z}\exp\left(\frac{-E_i}{kT}\right)\right]P_{tr}(E_i \to E_j), \quad (9)$$

where the overall rate ν_{Pr} must be a function of temperature, and the quantity in square brackets is the Boltzmann-distribution fractional occupancy of the initial state at that temperature. Equation (8) is required to preserve the overall Boltzmann distribution (and hence the state of equilibrium in the system at constant, well-defined temperature T) of level occupations over the course of many fluctuations. In a finite cluster, these fluctuations necessarily result in some jitter in the level occupations around the best equilibrium values, but the effect is reduced by increasing the size of the cluster (although that increases the computer time needed to run a simulation).

Reproduction of the μSR line shapes observed in PrP_x requires $kT < E_1$, in which case only a small fraction of the Pr are excited at any instant. In that case, the cluster must be made large enough that the average number of ions excited in the whole cluster is not small. The lower kT/E_1 gets, the larger the cluster must be to assure this. To accommodate the lowest kT/E_1 ($\sim$0.18) needed to reproduce our data, a cube of 30 unit cells on a side, thus containing 15 376 Pr ions, was used, producing an average of nearly 60 ions (0.4%) in excited states at any instant in the cluster at that temperature. This number again emphasizes the magnetically dilute situation in PrP. Returning to the simulation of an individual fluctuation, once a new level has been chosen for the ion, if it is E_1 or E_3, the moment direction is assigned randomly. The new field at the muon due to this one fluctuation is calculated, and the muon spin precesses in this new field until the next fluctuation occurs.

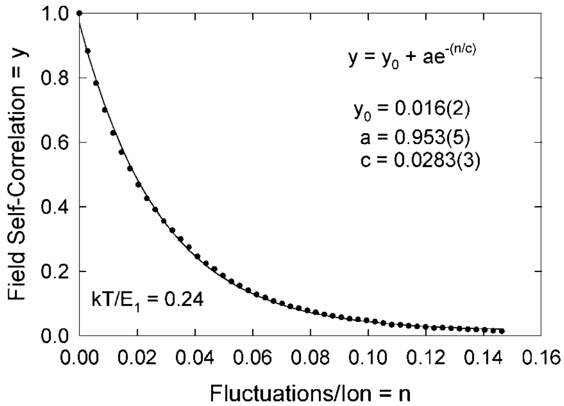

Figure 8. Muon-site field self-correlation $\langle \hat{\mathbf{B}}(0) \cdot \hat{\mathbf{B}}(n) \rangle$ as a function of the number of fluctuations/ion n in the Monte Carlo CEF-state fluctuation model of PrP for $kT/E_1 = 0.24$. The solid curve is the least-squares fit to the equation shown.

4. Results of the simulations

One bonus of the detailed nature of the simulation is a first look at the connection between the ion fluctuation rate and the correlation time of the local field at the muon site. Fits of strong-collision-dynamic Kubo–Toyabe relaxation functions to μSR data produce values of the 'fluctuation rate of the local field at the muon' ν_{hop}, which in this context is better thought of as the reciprocal of the correlation time of the local field, characterizing the strong-collision model's exponential decay of the self-correlation of that field with time. Before a comparison of the simulations to the well-known strong-collision model behaviour is made, it should be verified that the Monte Carlo model does generate exponential decay of the local-field self-correlation with time. This is actually a check of whether the computer model, as we have implemented it, is physically reasonable. Since the local field is a vector, however, a number of correlations can be defined, and it is not clear which one is most appropriate to consider. A particularly simple one is

$$\langle \hat{\mathbf{B}}(0) \cdot \hat{\mathbf{B}}(t) \rangle = \left\langle \frac{\mathbf{B}(0) \cdot \mathbf{B}(t)}{|\mathbf{B}(0)|\,|\mathbf{B}(t)|} \right\rangle = \langle \cos[\theta(t)] \rangle , \tag{10}$$

where $\hat{\mathbf{B}}(t)$ is the unit vector in the direction of the magnetic field at time t and $\theta(t)$ is the angle between the initial local field and the field at time t. In fact, the simulations first provide this correlation as a function of the number of fluctuations since the muon stop, in which form it depends upon the value of $kT/|B_4|$ only, and does not depend on the fluctuation rate. An example is shown in figure 8. The solid curve on the figure is the fit of the near-exponential decay equation shown in the figure. There is only a slight deviation of the fit from the initial correlation, and a small offset from zero at late times. Similarly, we found that pure exponential decay fitted well the simulated correlation as a function of the number of fluctuations for all values of $kT/|B_4|$ for which we ran simulations. To obtain the correlation as a function of time (equation (10)), the numbers on the horizontal axis of figure 8 must be divided by the user-chosen value of ν_{Pr}. The parameter c in the figure is the number of fluctuations per Pr ion needed to drive the local-field correlation to 1/e, and therefore c/ν_{Pr} is the local-field self-correlation time ($\tau_{\mathrm{hop}} = 1/\nu_{\mathrm{hop}}$). When $kT/E_1 < 0.4$, the first excited level is the only one significantly occupied, and c was found to be almost exactly twice the fractional occupancy of that state (and that relation remains approximately true to much higher kT/E_1), but it is not clear to us why that is so.

The solid curves in figure 3 show the results of runs of the simulation program with parameters manually adjusted to approximate the data shown. For $\mathrm{PrP}_{0.9}$ at 4 K (the upper

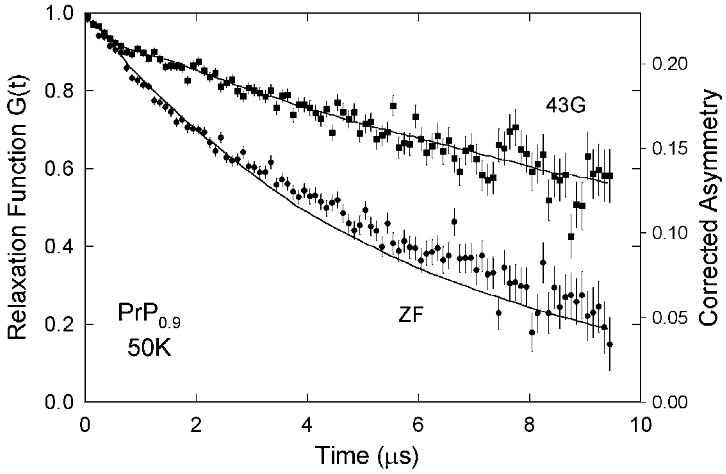

Figure 9. ZF and 43 G LF μSR asymmetry spectra at 50 K in $PrP_{0.9}$. The solid curves show Monte Carlo simulations of the CEF-state fluctuation model described in the text.

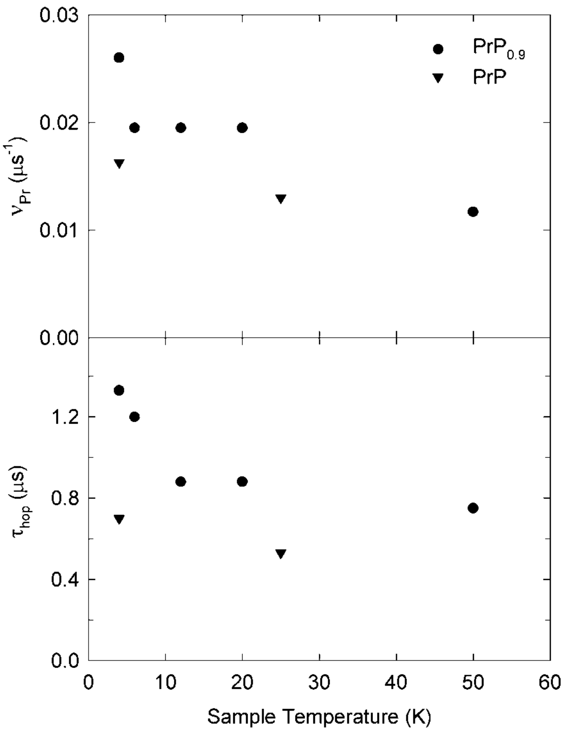

Figure 10. Temperature dependence of the Monte Carlo Pr fluctuation rate parameter deduced from matching simulations to PrP_x μSR data (upper panel), and of the resulting muon-site local-field self-correlation time (lower panel).

panel), the simulation parameters are $kT/E_1 = 0.25$ and $\nu_{Pr} = 0.026\ \mu s^{-1}$ (generating a local-field correlation time τ_{hop} of 1.33 μs), while for PrP at 4 K (lower panel) $kT/E_1 = 0.20$ and $\nu_{Pr} = 0.016\ \mu s^{-1}$ (for $\tau_{hop} = 0.70\ \mu s$). To demonstrate the range of behaviour observed, figure 9 shows ZF and 43 G LF μSR in $PrP_{0.9}$ at 50 K, together with simulation lines corresponding to $kT/E_1 = 0.19$ and $\nu_{Pr} = 0.012\ \mu s^{-1}$ (implying $\tau_{hop} = 0.75\ \mu s$). Figure 10 shows the temperature dependence of the Pr fluctuation rate ν_{Pr} deduced by manually adjusting the Monte Carlo parameters to match observed PrP_x data, and the temperature dependence of the resulting self-correlation time τ_{hop} of the local field at the muon site. Figure 11 similarly

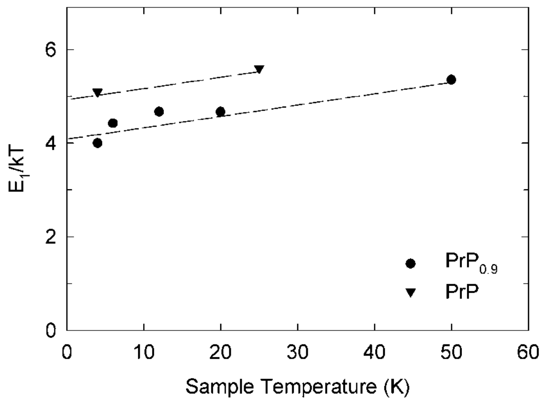

Figure 11. Temperature dependence of the Monte Carlo Pr first-excited-state energy divided by kT deduced from matching simulations to PrP_x μSR data. The dashed lines are guides for the eye. See the text for interpretation of this in terms of an exchange-induced approach to magnetic freezing.

shows the deduced temperature dependence of the first-excited-state energy divided by kT (that is, the reciprocal of the kT/E_1 parameter). Because of the crudeness of the parameter-adjustment procedure, the plots are 'low resolution', and reasonable error bars cannot be assigned to the points. The first thing to notice about figures 10 and 11 is that only a small range of model parameter values is used to span the observed behaviour from 50 K down to 4 K, a factor of more than ten in temperature. If figure 11 is taken literally, it implies that the energy of the first excited state is not independent of temperature, as normally expected, but instead varies nearly linearly with temperature. In $PrP_{0.9}$, at a measuring temperature of 50 K, the first excited state appears to be around 250 K, while in the same sample at 4 K, it appears to be only near 16 K. Since the first excited state is magnetic, this could be mode softening due to the exchange interaction (not included in the modelling) attempting to induce magnetic order, as seen in singlet ground-state praseodymium metal as a function of pressure [29] or alloying [30], and insulating $LiTbF_4$ doped with yttrium [31–34]. In magnetic mode softening, what would normally be a single-ion (dispersionless) magnetic CEF level above a non-magnetic ground state becomes, because of the exchange coupling between ions, a collective 'exciton' with a dispersion relation, and the minimum energy of this dispersion relation (which governs the onset of fluctuations, and thus is mimicked by E_1 of our more simplistic model) goes to zero at the magnetic ordering transition. In the application of our model to the PrP_x data, E_1 always remains greater than kT, so, in this speculation, the material attempts to set up magnetic order but does not quite succeed. The apparent increase in Pr fluctuation rate as the temperature decreases might be a reality if in fact the minimum energy of the dispersion relation was decreasing rapidly with temperature. The difference between PrP and $PrP_{0.9}$ appears to be that the minimum of the dispersion relation is about 20% higher in energy in PrP than it is in $PrP_{0.9}$ at the same temperature (and the Pr fluctuation rate is a bit lower). These, however, are rather speculative conclusions to draw from the amount of data available, a simulation model that does not yet explicitly incorporate exchange effects, and the narrow range of simulation parameters involved.

The fluctuation rate ν_{Pr} is surprisingly low, particularly as the temperature rises to 50 K. Normally, a substantial increase in fluctuation rate with temperature is to be expected as the density of phonons increases. If one accepts the simple interpretation of figure 10, that the energy of the first excited state (interpreted as a temperature-dependent exciton) rises almost linearly with temperature, so that the ratio E_1/kT remains nearly constant and greater than one, then a nearly-constant fluctuation rate is reasonable. That simple interpretation of figure 10, however, is one of the results of this modelling that is most difficult to believe. Also, note that rotation of the Pr spin when in the triplet states has been ignored: the Pr spin has been assumed static when it is not zero. It is not clear how Pr-spin rotation should be modelled in this context without needing to make a variety of arbitrary assumptions and introducing at least one new adjustable parameter, the Pr triplet spin-rotation rate (the fluctuation rate $\nu_{\rm Pr}$ is the spin–lattice fluctuation rate, corresponding to the spin–lattice relaxation time T_1, while this new parameter would be the spin–spin fluctuation rate, corresponding to the spin–spin relaxation time T_2). Any such addition to the model would provide a new, though weak, relaxation channel, and would increase the rate of muon spin relaxation predicted for fixed values of the current parameters (for an example of this sort of effect in simpler circumstances, see [7]). Then, to fit our observed data, it would be necessary to reduce the deduced values of $\nu_{\rm Pr}$ from their already surprisingly low values.

5. A different, unsuccessful, model

In the 'induced-moment spin glass' model introduced by Hasanain *et al* [1], the presence of a P vacancy beside a Pr ion shifts the Pr CEF levels, producing a magnetic ground state for that ion. Such a vacancy definitely destroys the cubic symmetry at the Pr site, and should be expected to introduce quadrupole (B_2^0 at least) and new higher-order terms in the CEF Hamiltonian. Just adding an axial quadrupole (B_2^0) term to the cubic terms, as Hasanain *et al* do for demonstration purposes, results in individually-moving singlets as the lowest states, for which stable magnetic moments would only be found by explicit consideration of exchange, which is beyond the scope of this work. To provide a comparison Monte Carlo model approaching the induced-moment model, an independent set of calculations was run using the same CEF-state fluctuation calculation, but with a small fraction of Pr ions selected at random in each cluster having a magnetic moment in the ground state, and no moment in excited states. For simplicity, and to see clearly the effect of these fluctuating moments, the rest of the ions in the cluster were made non-magnetic. Combining these two models, which might seem more realistic, would result in an unmanageably large parameter space to explore. By itself, this model has one additional user-controlled parameter that the previous model does not: the fraction of Pr ions that are magnetic.

The relaxation functions produced by this alternate model did not come close to reproducing the PrP_x data for any set of parameters attempted. Again, the difference in behaviour between placing the muon in the interstitial site or the P-vacancy site was small. For magnetic fractions small enough to produce a Lorentzian field distribution at the muon site and sufficiently fast fluctuations for a monotonic ZF relaxation function, that function was approximately root-exponential, and applied-LF relaxation functions were similar to those predicted by [22], i.e., it roughly reproduced the unacceptably poor fits of figure 5. The novelty of switching ion moments on and off (rather than just re-orienting them) is not enough to generate strong-collision dynamics on the Lorentzian distribution at the muon site when those ions are dilute and fixed in position. At slightly higher magnetic-ion concentrations, the two-apparent-site field distribution behaviour described in [10] appears, causing a non-monotonic wiggle at early times in each ZF relaxation function, and that is not seen in the PrP_x data. When the magnetic-ion concentration is high enough to return to a single-apparent-site field distribution, the distribution is nearly Gaussian, and while the fast-fluctuation ZF relaxation function is then exponential (with relaxation rate approaching $\lambda_{\rm G,ZF} = -2\Delta^2 t/\nu_{\rm hop}$, where $\Delta = \gamma_\mu B_{\rm rms}$), it decouples in LF approximately in the well-known dynamic-Gaussian manner, equation (4). The PrP_x data obey equation (7) instead. Combining this model for a few Pr moments with the other model for all the other spins would only serve to change the previous model's line shapes, which fit the PrP_x data at individual temperatures, toward line shapes that will not fit any of the data, with little chance of allowing a clearer physical understanding of the temperature dependence of the data.

6. Other models?

In trying to explain unusual μSR results in other praseodymium materials, researchers have proposed muon-induced effects. With such an effect operating, muons are no longer a benign probe species, because they are noticeably disturbing the sample's behaviour. For example, in $PrNi_5$ [35] and $PrIn_3$ [36], it was argued that the muon's charge changes the CEF splittings of nearby Pr ions. We have not been able to construct any muon-induced effect model that explains our observations in PrP_x. In this section we describe a possible alternate explanation that we have considered, and dismissed.

In our preferred model described above, the dynamics are entirely Pr-ion spin dynamics, with a stationary muon. We noted that muons do move measurably in some materials, but argued that with substantial disorder as in intentionally vacancy-riddled materials such as $PrP_{0.9}$, such motion is unlikely. Unfortunately, it is also difficult to prove the absence of motion when the relaxation function is dynamic due to spin fluctuations. So, could a muon-motion model explain our data? We need to have a fluctuation rate that remains non-zero (though not large) down to low temperatures. This suggests tunnelling rather than thermally-activated hopping. It could be localized, or in principle it could be over long ranges, when it is often called 'quantum diffusion'. Muon quantum diffusion has only been observed in pure materials, with defects causing trapping that interferes with the diffusion, so that seems unlikely here. On the other hand, even with vacancies present, localized tunnelling is conceivable. Perhaps when the muon sits in a vacant phosphorus site, the Pr ions are unaffected (have singlet ground states), but when the muon moves (by tunnelling) to an adjacent interstitial position, it changes the CEF levels of the nearest one or two Pr ions so much that they gain magnetic moments (and then when the muon moves back to the vacancy, the moments switch off again). Problems with this model include (a) it is difficult to generate a Lorentzian field distribution, because at low temperature there should be either no field at the muon site, or a large field, nothing in between (in fact, on-off local field fluctuation like this has been proposed as the cause of a different relaxation function: 'undecoupleable Gaussian relaxation' in Kagomé lattice materials [37]), and (b) it is difficult to explain the composition dependence of the measured field distribution width. Instead, one would expect the distribution width to be composition independent, but as the vacancy density drops, muons that fail to find any vacancy should generate a new signal that would reduce the asymmetry of the tunnelling, moment-switching signal, partially replacing it with a 'pristine material' signal that would be non-relaxing at low temperatures. That is not what we see.

7. Conclusions

To draw conclusions from our PrP μSR results that are not excessively model dependent, we must choose our path of argument carefully. As we see it:

(1) The ZF and LF-μSR data for both PrP and $PrP_{0.9}$ are well fitted by the strong-collision-dynamic Lorentzian Kubo–Toyabe relaxation function. The data are not fitted well at all by any well-known relaxation function that would outwardly seem reasonable, but that features motional narrowing.

(2) Monte Carlo modelling shows that fluctuations of all the praseodymium ions out of their CEF singlet ground states into magnetic excited states can reproduce the relaxation functions observed, complete with lack of motional narrowing. We attribute the failure

of the model to reproduce the temperature dependence of the relaxation to the lack of exchange interaction effects in the model.

(3) The fast-fluctuation-limit ZF strong-collision dynamic Lorentzian Kubo–Toyabe relaxation rate depends only on the hwhm of the field distribution, and not on the detailed value of any fluctuation rate (as long as $\nu_{hop} \gg a$). Changes in the ZF relaxation rate then cannot be due to changes in fluctuation rates; they can only be due to change in the size of the typical fields at the muon site.

(4) Therefore, the observed increase of ZF relaxation rate as the temperature is reduced in both materials indicates that the typical local fields are increasing as the temperature is reduced, in both materials. Both materials are becoming stronger paramagnets as the temperature decreases. This is exactly the opposite effect to that expected for a singlet ground-state system with no exchange interaction.

(5) (Speculation). The exchange interaction moving the system toward magnetic ordering or freezing could produce the increases in ZF relaxation rate seen as temperatures are reduced, because exchange makes materials more magnetic as the transition temperature is approached from above. It is not clear in these cases if there is a magnetic transition temperature greater than or equal to zero. If there was a transition, the increases in ZF relaxation rates as the temperature decreases would be candidates for discussion in terms of critical effects. The Monte Carlo model mimics this when it reproduces the temperature dependence by reducing the first-excited-state energy as the temperature decreases, in apparent magnetic 'mode softening'. Perhaps exchange can produce these effects even if it is not quite strong enough to actually cause a magnetic transition.

In conclusion, then, μSR and bulk magnetization data have been presented for the singlet ground-state systems PrP and $PrP_{0.9}$. Contrary to assertions in the literature, no spin-glass freezing is observed in either material down to dilution-refrigerator temperatures. The ZF and LFμSR data were found to have the form of the strong-collision-dynamic Lorentzian Kubo–Toyabe relaxation function at all temperatures measured (60 mK–50 K), once the form of the fast-fluctuation-limit LF decoupling (equation (7)) was established. A Monte Carlo model has been constructed that shows that fluctuations of the Pr ions out of their CEF singlet ground states into their magnetic excited states (and back down again) produce the strong-collision-dynamic Lorentzian relaxation functions observed. The failure of the second model, where only a small fraction of the Pr ions could ever be magnetic, shows that the majority of the Pr ions in each sample must be magnetic part of the time (and have zero moment at other times) to offer every muon access to the complete Lorentzian distribution of local fields, a necessary condition for strong-collision dynamics. The (more successful) model is of a purely paramagnetic state, and no magnetic exchange between Pr ions is included. The increase in ZF relaxation rate as the temperature decreases, in both samples, seems to indicate that exchange causes an approach to magnetic freezing, but the process is left incomplete, even at the lowest temperatures.

Explicitly modelling the dynamics of the local field at the muon site allows inspection of details not highlighted in usual treatments of dynamics. The fact that the field is a vector function of time means that there is not a unique scalar self-correlation of the local field as a function of time, although $\langle \cos[\theta(t)] \rangle$, where $\theta(t)$ is the angle between the local field at the instant the muon stops and the local field at a later time t, is clearly an interesting correlation to watch. For the CEF singlet ground fluctuations modelled here (on-off flickering, not the usual form of moment fluctuation, which is rotation), this local-field self-correlation exhibits a correlation time τ_μ that is very close to the fractional occupation of the Pr first exited state divided by the Pr fluctuation rate ν_{Pr}.

Acknowledgments

This work was supported in part by the US Air Force Office of Scientific Research, the Swedish Science Research Council, and the BMBF of Germany.

References

[1] Hasanain S K, Guertin R P, Westerholt K, Guyot M and Foner S 1981 *Phys. Rev.* B **24** 5165
[2] Yoshizawa H, Shapiro S M, Hasanain S K and Guertin R P 1983 *Phys. Rev.* B **27** 448
[3] Noakes D R, Wäppling R, Kalvius G M, Andersson Y, Broddefalk A, White M F and Stronach C E 2000 *Physica* B **289/290** 303
[4] Cox S F J 1987 *J. Phys. C: Solid State Phys.* **20** 3187
[5] Lee S L, Kilcoyne S H and Cywinski R (ed) 1999 *Muon Science* (London: Institute of Physics Publishing)
[6] Kalvius G M, Noakes D R and Hartmann O 2001 *Handbook on the Physics and Chemistry of Rare Earths* vol 32, ed K A Gschneidner, L Eyring and G H Lander (Amsterdam: Elsevier) p 55
[7] Noakes D R, Brewer J H, Harshman D R, Ansaldo E J and Huang C Y 1987 *Phys. Rev.* B **35** 6597
[8] Schenck A and Gygax F N 1995 *Handbook of Magnetic Materials* vol 9, ed K H J Buschow (Amsterdam: Elsevier) p 57
[9] Mikaelyan A L and Smilga V P 1981 *Sov. Phys.—JETP* **53** 1216
[10] Noakes D R 1991 *Phys. Rev.* B **44** 5064
[11] Kehr K W, Honig G and Richter D 1978 *Z. Phys.* B **32** 49
[12] Hayano R S, Uemura Y J, Imazato J, Nishida N, Yamazaki T and Kubo R 1979 *Phys. Rev.* B **20** 850
[13] Luke G M, Brewer J H, Kreitzman S R, Noakes D R, Celio M, Kadono R and Ansaldo E J 1991 *Phys. Rev.* B **43** 3284
[14] Kubo R and Toyabe T 1966 *Magnetic Resonance and Relaxation* ed R Blinc (Amsterdam: North-Holland) p 810
[15] Kubo R 1981 *Hyperfine Interact.* **8** 731
[16] Slichter C P 1978 *Principles of Magnetic Resonance* (Berlin: Springer)
[17] Uemura Y J 1982 *PhD Thesis* University of Tokyo
[18] Uemura Y J 1981 *Hyperfine Interact.* **8** 739
[19] Uemura Y J, Yamazaki T, Hayano R S, Nakai R and Huang C Y 1981 *Phys. Rev. Lett.* **45** 583
[20] Uemura Y J 1980 *Solid State Commun.* **36** 369
[21] Uemura Y J, Yamazaki T, Harshman D R, Senba M and Ansaldo E J 1985 *Phys. Rev.* B **31** 546
[22] Keren A 1994 *Phys. Rev.* B **50** 10039
[23] Brewer J H, Crowe K M, Gygax F N and Schenck A 1975 *Muon Physics* vol 3, ed V W Hughes and C S Wu (New York: Academic) p 3
[24] Brewer J H 1983 unpublished
[25] Hartmann O, Karlsson E, Wäppling R, Richter D, Hempelmann R, Schulze K, Patterson B, Holzschuh E, Kündig W and Cox S F J 1983 *Phys. Rev.* B **27** 1943
[26] Fulde P and Loewenhaupt M 1985 *Adv. Phys.* **34** 589
[27] Lea K R, Leask M G M and Wolf W P 1962 *J. Phys. Chem. Solids* **23** 1381
[28] Noakes D R 1999 *J. Phys.: Condens. Matter* **11** 1589
[29] McEwen K A, Stirling W G and Vettier C 1983 *Physica* B **120** 152
[30] Lebech B, McEwen K A and Lindgård P A 1975 *J. Phys. C: Solid State Phys.* **8** 1684
[31] Youngblood R W, Aeppli G, Axe J D and Griffin J A 1982 *Phys. Rev. Lett.* **49** 1724
[32] Kötzer J, Neuhaus-Steinmetz H, Froese A and Görlitz D 1988 *Phys. Rev. Lett.* **60** 647
[33] Grahl M and Kötzer J 1992 *J. Magn. Magn. Mater.* **104–107** 219
[34] Marx C, Görlitz D and Kötzer J 1996 *Phys. Lett.* A **210** 141
[35] Feyerherm R, Amato A, Grayevsky A, Gygax F N, Kaplan N and Schenck A 1995 *Z. Phys.* B **99** 3
[36] Tashma T, Amato A, Grayevsky A, Gygax F N, Pinkpank M, Schenck A and Kaplan N 1997 *Phys. Rev.* B **56** 9397
[37] Uemura Y J, Keren A, Kojima K, Le L P, Luke G M, Wu W D, Ajiro Y, Asano T, Kuriyama Y, Mekata M, Kikuchi H and Kakurai K 1994 *Phys. Rev. Lett.* **73** 3306